

Reduced Equalization Needs of 100 GHz Bandwidth Plasmonic Modulators

Benedikt Baeuerle , Wolfgang Heni , Claudia Hoessbacher , Yuriy Fedoryshyn, Arne Josten , Christian Haffner , Tatsuhiko Watanabe , Christopher Uhl , Horst Hettrich, Delwin L. Elder , Larry R. Dalton , Senior Member, IEEE, Michael Möller, and Juerg Leuthold , Fellow, IEEE

Abstract—As bit rates of optical interconnects increase, a large amount of complicated signal conditioning is needed to compensate for the insufficient bandwidth of current modulators. In this paper, we evaluate the reduced equalization requirements of high-bandwidth plasmonic modulators in short-reach transmission experiments. It is shown that transmission of 100 Gbit/s non-return-to-zero (NRZ) and 112 Gbit/s pulse-amplitude modulation-4 over 1 km and 2 km distance is possible without any receiver equalization. At higher bit-rates, such as 120 Gbit/s NRZ, data transmission is demonstrated over 500 m with reduced receiver equalization requirements. Transmission up to 200 Gbit/s over 1 km is also shown with more complex receiver equalization. The reduced complexity of the receiver digital signal processing is attributed to a flat frequency response of at least 108 GHz of the plasmonic modulators. All single wavelength transmissions have been performed at 1540 nm in standard single mode fiber.

Index Terms—Direct detection, electro-optic devices, electro-optic modulation, integrated optics, optical interconnects, optical modulation, optical transmitter, plasmonics, silicon photonics.

I. INTRODUCTION

HIGH-SPEED electro-optic (EO) modulators are an essential component in today's communication network that connects electrical information processing with the optical information transport. A large EO modulation bandwidth in combination with a small footprint, low driving voltages and a simple

Manuscript received November 26, 2018; revised January 24, 2019; accepted January 29, 2019. Date of publication February 4, 2019; date of current version April 11, 2019. This work was supported in part by EU-project PLASMOfab under Grant 688166, in part by ERC PLASILOR under Grant 670478, in part by NSF under Grant DMR-1303080, and in part by AFOSR under Grant FA9550-15-1-0319. (*Corresponding author: Benedikt Baeuerle.*)

B. Baeuerle, W. Heni, C. Hoessbacher, Y. Fedoryshyn, A. Josten, C. Haffner, T. Watanabe, and J. Leuthold are with the ETH Zurich, Institute of Electromagnetic Fields (IEF), 8092 Zurich, Switzerland (e-mail: bbaeuerle@ethz.ch; wheni@ethz.ch; choessbacher@ethz.ch; yuriy@ief.ee.ethz.ch; ajosten@ethz.ch; haffnerc@ethz.ch; tatsuhiko.watanabe@ief.ee.ethz.ch; juerg.leuthold@ief.ee.ethz.ch).

C. Uhl is with Saarland University, Chair of Electronics and Circuits, 66123 Saarbrücken, Germany (e-mail: christopher.uhl@eus.uni-saarland.de).

H. Hettrich is with MICRAM Microelectronic GmbH, 44801 Bochum, Germany (e-mail: horst.hettrich@micram.com).

D. L. Elder and L. R. Dalton are with the University of Washington, Department of Chemistry, Seattle, WA 98195-1700 USA (e-mail: elderdl@uw.edu; dalton@chem.washington.edu).

M. Möller is with Saarland University, Chair of Electronics and Circuits, 66123 Saarbrücken, Germany, and also with MICRAM Microelectronic GmbH, Bochum 44801, Germany (e-mail: m.moeller@mechatronik.uni-saarland.de).

Color versions of one or more of the figures in this paper are available online at <http://ieeexplore.ieee.org>.

Digital Object Identifier 10.1109/JLT.2019.2897480

and cost-efficient receiver design are the key design parameters for EO modulators to enable the next generation of optical communication systems. This is a prerequisite to mitigate the capacity bottleneck between electrical and optical interfaces and to remedy their disparity [1].

Such EO modulators are required for transceivers with intensity-modulation and direct-detection (IM/DD) in short-reach optical interconnects where transmission distance of 100 m and up to 2 km are bridged and low complexity is of significant importance. To optimize the cost efficiency of such transceivers, the number of parallel lanes should be kept minimal to decrease the amount of optical components. Therefore, modulator bandwidths in the range of 100 GHz are desired to allow for data rates beyond 100 Gbit/s OOK per single lane [2]. Furthermore, to enable a cost effective dense integration and parallelization on limited chip space the foot print of modulators has to be reduced significantly, preferably to the micrometer scale [3]. Moreover, driving voltages of such modulators should be kept below one volt to avoid power hungry driver amplifier electronics and to enable most compact integration [4].

A broad range of modulator technologies has already convincingly demonstrated at least 100 GBd short-reach data transmission. For instance, electro-absorption modulators (EAM) enable modulation at the micrometer scale and direct integration with a distributed feedback laser (DFB) [5]. 100 GBd modulation has been demonstrated on both the silicon based GeSi technology platform [6] and on the InP technology platform [5], [7]. However, the absorption modulation leads inherently to a trade-off between extinction ratio and signal chirping. Conversely, Mach-Zehnder modulators (MZMs) allow for pure amplitude modulation in the push-pull configuration with a large extinction ratio and no additional chirp. Data rates of up to 300 Gbit/s have been demonstrated [8]. MZMs have been implemented on several technology platforms like LiNbO₃ [9]–[12], InP [8], [13], silicon-organic hybrid (SOH) [14], and polymer photonics [15]. Nevertheless, the dimensions of such modulators are limited to the millimeter scale.

An alternative to these established technologies is the plasmonic-organic hybrid (POH) approach [16]. It combines MZM-enabled pure amplitude modulation at the micrometer scale [17], [18], large extinction ratios of more than 25 dB [19], an electro-optic bandwidth of at least 170 GHz [20], and 100 GBd non-return-to-zero (NRZ) OOK modulation with driving voltages below 1 V_{pp} [21]. Furthermore, the POH technology

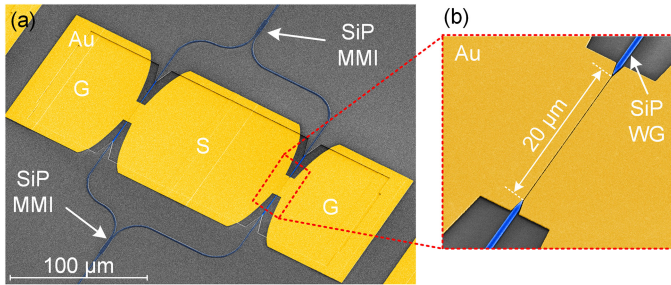


Fig. 1. Colorized scanning electron microscope picture of the plasmonic-organic hybrid Mach-Zehnder modulator. (a) A silicon photonics (SiP) Mach-Zehnder interferometer with two incorporated plasmonic phase shifters. The light is split and combined by SiP multi-mode interference (MMI) couplers. The electrical signal is applied via ground (G) – signal (S) – ground (G) pads. (b) Close-up picture of one of the phase shifters. The light is coupled from SiP waveguides (WG) into the gold (Au) slot waveguide. An organic electro-optic material in the slot waveguide allows for a phase shift depending on the drive voltage.

has been demonstrated for dense integration in an optical transmitter with parallel channels [22]–[24]. Yet, it is unclear if the flat frequency response of POH modulators brings an advantage in short-reach optical transmission systems by e.g., offering a reduced receiver complexity.

In this paper, we show that plasmonic intensity modulators offer reduced receiver DSP requirements in short-reach optical interconnect links with direct detection at a wavelength of around 1540 nm. We first measure an electro-optic bandwidth beyond 108 GHz. We then analyze the complexity of the receiver DSP for different interconnect scenarios. First, transmission with line rates of 100 Gbit/s NRZ OOK, 112 Gbit/s PAM-4, and 120 Gbit/s NRZ are shown through 2 km, 4 km, and 500 m long standard single mode fibers (SMF) with BERs below the KP4 FEC threshold of 2.4×10^{-4} [25]. Ultimately, 200 Gbit/s PAM-4 data transmission is performed through a 1 km long standard SMF with a BER below 7.5×10^{-3} . The experiments reveal that no equalization is needed for transmission of 100 Gbit/s (NRZ) and 112 Gbit/s (PAM-4) over 1 km and 2 km and a HD-FEC threshold of 3.8×10^{-3} can be maintained.

The paper is based on initial results published previously at CLEO'2018, see Ref. [26].

II. PLASMONIC ORGANIC HYBRID MODULATOR

Fig. 1 depicts the colorized scanning electron microscope (SEM) picture of the plasmonic-organic hybrid modulator [19] used for the optical transmission experiments. The POH modulator technology combines plasmonic waveguide structures [16], which confine the light to the subwavelength scale, with pure phase modulation enabled by the linear electro-optic Pockels-effect in an organic electro-optic material [27]. The optical carrier is coupled to silicon photonic (SiP) waveguides on the chip via silicon grating couplers (GCs) [28] adapted for non-perpendicular incidence. Intensity modulation is achieved by two plasmonic phase modulators (PPMs) [29] integrated into a silicon photonics Mach-Zehnder interferometer (MZI). Light is split and combined by silicon photonic multimode interference (MMI) couplers. The plasmonic phase modulator is a metal

insulator metal (MIM) slot waveguide filled with an organic electro-optic material (HD-BB-OH/YLD124) [30]. The metallic waveguide is made of gold and additionally functions as contact electrodes. This enables small RC time constants and therefore an electro-optic bandwidth of more than 170 GHz [20], [31]. Applying a voltage between the electrodes leads to a change of the refractive index of the organic electro-optic material due to the Pockels electro-optic effect. This results in phase modulation of the plasmonic mode. Amplitude or intensity modulation is achieved by the MZI structure.

In the experiments we used two devices. The first device features 20 μm long and ~ 140 nm wide plasmonic slot waveguides. The on-chip insertion losses are ~ 15.5 dB with additional fiber-to-chip coupling losses of ~ 8 dB (grating coupler loss: 4 dB/coupler) and a V_π of ~ 8.5 V. The second device features 25 μm long and ~ 130 nm wide slot waveguides. The on-chip insertion losses are ~ 17.5 dB with additional fiber-to-chip coupling losses of ~ 10 dB (grating coupler loss: 5 dB/coupler) and a V_π of ~ 7 V. The devices are fabricated in-house on a silicon-on-insulator (SOI) platform [19].

In the future, device performance can be improved by more efficient electro-optic materials. The plasmonic-organic hybrid slot waveguide structure allows the flexibility to integrate various organic electro-optic materials into the slot [27]. It has been demonstrated that the non-linear coefficient of such organic electro-optic materials can be improved by at least a factor of two [32], [33]. Consequently, just by integrating better nonlinear materials into the modulator smaller V_π can be achieved. Conversely, at the cost of a constant V_π the active area can be shortened and therefore the insertion losses can be reduced. Furthermore, long-term thermally stable organic electro-optic materials with a high non-linear coefficient have been demonstrated in MZM devices [34].

III. EXPERIMENTAL SETUP

The plasmonic-organic hybrid (POH) Mach-Zehnder modulator (MZM) is implemented in a short-reach transmission testbed to evaluate its performance in an optical interconnect scenario. Fig. 2 depicts the experimental setup. It comprises three parts, which are the intensity modulation (IM) transmitter, the fiber channel, and the direct detection (DD) receiver.

In the IM transmitter, two different scenarios are implemented, which can be mainly distinguished by the electrical signal generation. The first scenario Tx-A comprises a Micram digital-to-analog converter (DAC) [35] with a sampling rate of 100 GSa/s and an electrical 3 dB bandwidth of 42 GHz for analog waveform generation. The digital waveform is generated offline beforehand. This comprises the generation of a random bit sequence, Gray mapping on symbols and pulse shaping with a square-root-raised-cosine with a roll-off factor of 0.4 in the case of PAM-4. In the case of 100 Gbit/s NRZ signals, only the generation of a random bit sequence is required. Furthermore, we applied pre-distortion to compensate for linear and non-linear impairments [36] from the electronic devices and cables based on electrical back-to-back measurements. In the second transmitter scenario Tx-B, the signal generator is replaced by

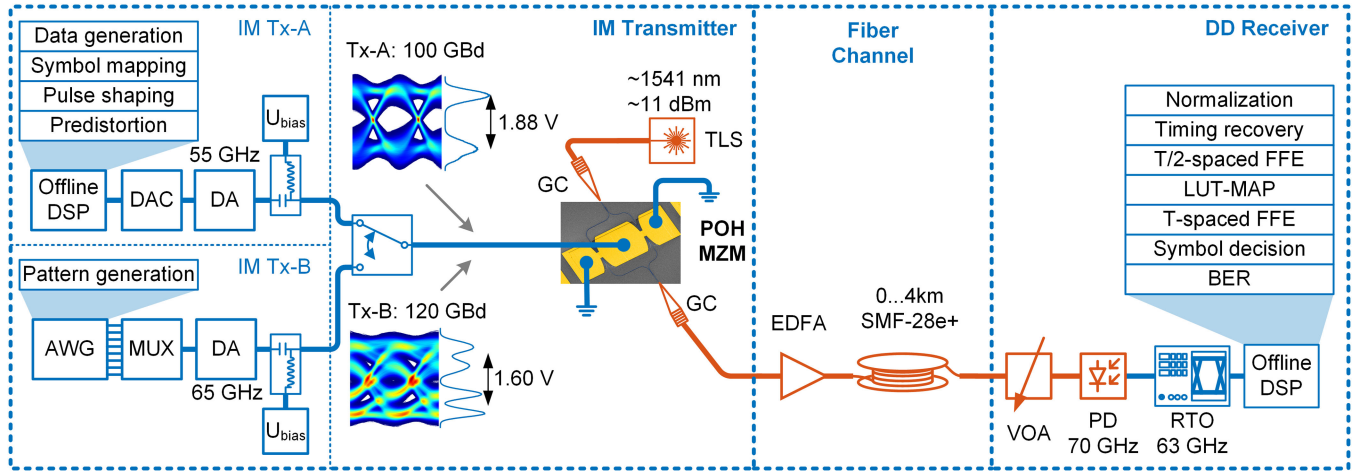


Fig. 2. Experimental setup. The intensity modulated (IM) transmitter with two electronic driver scenarios. In the first scenario Tx-A, the electrical signal is generated with a digital-to-analog converter (DAC) and offline digital signal processing (DSP) with symbol rates of up to 100 GBd. In the second scenario Tx-B, a 120 GBd signal is generated by an electronic multiplexer, which is fed by eight decorrelated 15 GBd bit streams generated by an arbitrary waveform generator (AWG). The electrical signal is amplified by driver amplifiers (DAs). The electrical signal is fed to the plasmonic-organic hybrid Mach-Zehnder modulator. A tunable laser source (TLS) generates the optical carrier and applied via grating couplers (GC) onto the modulator chip. The optical signal is amplified by an erbium doped fiber amplifier (EDFA) and transmitted through a single mode fiber (SMF). At the direct detection (DD) receiver, a variable optical attenuator (VOA) defines the received optical power level and a photodiode (PD) detects the optical signal. The electrical signal is digitized by a real-time oscilloscope (RTO) and offline DSP evaluates the data using feed-forward equalization (FFE) and look-up table (LUT) based maximum a posterior (MAP) equalization.

an electronic multiplexer to achieve larger symbol rates. The multiplexer [37] is realized in SiGe BiCMOS technology. It requires eight decorrelated 15 GBd bit streams generated by an arbitrary waveform generator at the input and generates a 120 Gbit/s NRZ signal. The outputs of the transmitters Tx-A and Tx-B are amplified by broadband driver amplifiers (DA) with 3 dB bandwidths of 55 GHz (SHF 807) and 65 GHz (SHF 827). The driver amplifier with a 65 GHz bandwidth has been used for Tx-B to address the larger bandwidth of the 120 Gbit/s NRZ signal. A bias tee is used to adjust the operating point. For the two scenarios, we measured root mean square voltages V_{rms} of 0.94 V and 0.80 V. The voltages were measured at 50Ω termination with a 63 GHz real-time oscilloscope just before the modulator chip. In Fig. 2, it can be seen that twice the V_{rms} , which is highlighted by arrows, aligns with the mean voltage swing at the maximum eye-opening of the two-level signals. The electrical signals are then applied via microwave probes to the on-chip POH MZM. The optical carrier is generated by a tunable laser source (TLS) at around 1540 nm with an optical power of 11 dBm. It is fed via grating couplers to the chip. Before transmission, the signal is optically amplified by an erbium doped fiber amplifier (EDFA) without an optical bandpass filter. The EDFA's input power is between -16.5 dBm and -12.5 dBm and the output power between 10 dBm and 12 dBm.

The transmission line comprises different spans of 100 m, 500 m, 1 km, 2 km, 3 km, and 4 km of SMF28e+ type standard single mode fiber (SSMF).

At the DD receiver, a variable optical attenuator (VOA) is used to adjust the signal for different receiver power levels. The optical signal is detected by a photodiode with a bandwidth of 70 GHz, which is directly attached to a real-time oscilloscope (RTO) to digitize the waveform. The RTO has an electrical bandwidth of 63 GHz and a sampling rate of 160 GSa/s. The

digitized signal is then analyzed by offline digital signal processing (DSP). The offline DSP comprises signal normalization, timing recovery, T/2-spaced feed-forward equalization (FFE) with a least mean square (LMS) update rule, a look-up table (LUT) based maximum a-posteriori (MAP) equalizer [38]–[40], a T-spaced FFE with LMS update rule, hard symbol decision, and error counting to calculate the bit error ratio (BER). The linear and nonlinear filters are trained in a data-aided mode over the first 10% to 25% of the received symbols and are applied afterwards statically.

IV. EXPERIMENTAL RESULTS

A. Electro-Optic Bandwidth

Firstly, we investigated the electro-optic bandwidth characteristics of the plasmonic modulator. The characterization includes two parts: the analysis with a broadband data signal for frequencies of up to 60 GHz and the assessment with a harmonic frequency signal between 10 GHz and 108 GHz.

For the evaluation with the broadband data signal, we used the experimental setup as mentioned above with the Tx-B scenario. We analyzed the electro-optic-electrical (EOE) frequency response derived by DSP from a 120 Gbit/s NRZ signal in an electrical and optical back-to-back (BTB) measurement. The electrical response corresponds to the NRZ signal as fed to the modulator. The optical BTB measurement includes the signal as generated in the modulator and received by the photodiode. The modulator response is then obtained by subtracting the electrical frequency response and photodiode response from the optical frequency response. To determine the frequency responses from the DSP equalizer of both the electrical and optical signals we used a T/2-spaced FFE with 101 taps and a data-aided LMS training procedure. This allowed us to derive the frequency

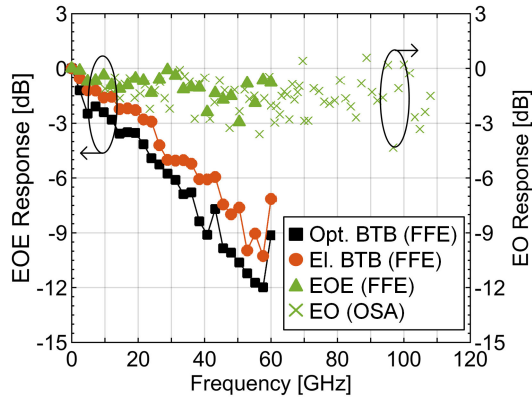


Fig. 3. Frequency responses as normalized magnitude versus frequency. The optical back to back (BTB) measurement in black (square). The electrical back-to-back (BTB) measurement in red (circle). The electro-optic (EO) bandwidth of a broadband signal in green (triangle) estimated with a feed-forward equalizer (FFE). The electro-optic bandwidth measured with an optical spectrum analyzer (OSA) in green (cross).

response for up to 60 GHz. Fig. 3 presents the results as normalized magnitude versus frequency for the optical (black squares) and the electrical (red circles) BTB measurements. The modulator response (green triangles) shows that there is no indication of a frequency roll-off of up to 60 GHz.

In the next step, we analyzed the electro-optical (EO) frequency response of the plasmonic modulator up to 108 GHz. We utilized heterodyne mixing of two tunable lasers in a photodiode to generate electrical harmonics of up to 108 GHz and applied them on the POH MZM. To evaluate the EO frequency response, we measured the ratio between optical carrier and modulated signal with an optical spectrum analyzer (OSA) [19] between 10 GHz and 108 GHz. We normalized this modulation efficiency and plotted it as normalized magnitude (green crosses) in Fig. 3. It can be seen that there is no indication of any magnitude roll-off for frequencies up to 108 GHz. The strong oscillations are related to the electrical back reflection from the device into the photodiode. The electro-optic bandwidth measurements are in good agreement with previous publications [20], [31].

B. Data Experiments

We present the bit error ratio (BER) performance at different received optical power levels for varying modulation formats, symbol rates, transmission distances and receiver DSP complexities. All measured BERs are calculated for $\sim 1.5 \times 10^7$ bits. With statistical confidence of at least 100 measured errors the minimal BER is around $\sim 9.5 \times 10^{-6}$. We consider three different input BER thresholds of hard-decision forward error correction codes as reference. The first code is known as KP4 FEC that is a Reed-Solomon RS(544,514) FEC code with a BER threshold of 2.4×10^{-4} [25]. The second code is known as HD-FEC. The HD-FEC is a FEC code with two interleaved Bose–Chaudhuri–Hocquenghem BCH(1020,988) codes with a BER threshold of 3.8×10^{-3} , an overhead of 7 %, and a net coding gain of 9.19 dB. It is defined by the OUT4 standard

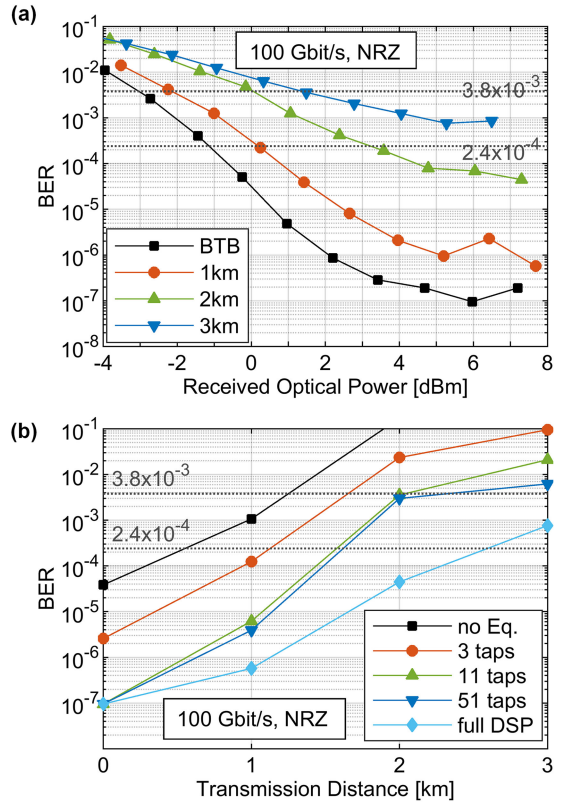


Fig. 4. Experimental results of 100 Gbit/s NRZ-OOK signals. As reference the FEC limits at 3.8×10^{-3} and 2.4×10^{-4} (grey dashed) are shown. (a) BER as a function of the received optical power for back-to-back (BTB) (black square), 1 km (red circle), 2 km (green triangle), and 3 km (blue triangle) transmission. (b) Complexity analysis of receiver DSP. BER as a function of the transmission distance for receiver DSP without any equalizer (black square), a T-spaced FFE with 3 taps (red circle), 11 taps (green triangle), 51 taps (dark blue triangle), and full DSP (light blue diamond).

G.975.1 [41], [42]. The third code is a hard decision staircase code with an overhead of 10 %, a net coding gain of 9.87 dB and a BER threshold of 7.54×10^{-3} [43].

Fig. 4(a) shows the BER results for 100 Gbit/s NRZ-OOK signals as a function of received optical power. The results are presented for back-to-back (BTB) and transmission spans between 1 km and 3 km. A 100 GBd data transmission for up to 2 km below the KP4-FEC limit and of up to 3 km below the HD-FEC is demonstrated. For this transmission experiment, a receiver DSP block with a T/2-spaced FFE with 51 taps, LUT-MAP with 5 taps, and a T-spaced FFE with 51 taps has been used. Fig. 4(b) shows the best achievable BER performance (i.e., at the optimum received powers, which are ~ 6 dBm, ~ 7.5 dBm, ~ 7.25 dBm, and ~ 6.5 dBm for BTB, 1 km, 2 km, and 3 km) for different transmission lengths and different receiver DSP complexities. We reduced the three equalizer stages to one single T-spaced FFE and varied the amount of filter taps. It can be seen, that no equalizer is needed to stay below a BER of 2.4×10^{-4} in the BTB scenario. For data transmission a T-spaced FFE with 3 taps, 11 taps, and the full DSP block were required for 1 km, 2 km, and 3 km of SMF. In the case of BTB and filter taps larger than 10 taps we measure only a single error which results

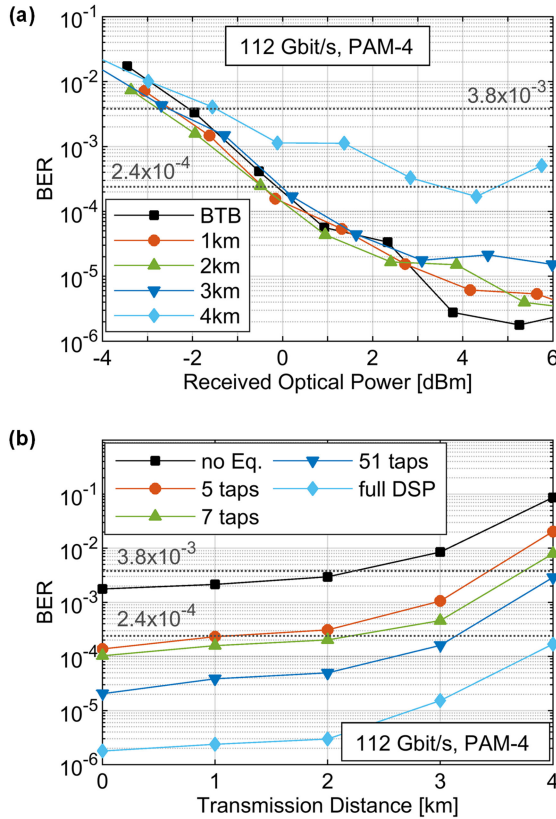


Fig. 5. Experimental results of 112 Gbit/s PAM-4 signals. As reference the FEC limits at 3.8×10^{-3} and 2.4×10^{-4} (grey dashed) are shown. (a) BER as a function of the received optical power for back-to-back (BTB) (black square), 1 km (red circle), 2 km (green triangle), 3 km (dark blue triangle), and 4 km (light blue diamond) transmission. (b) Complexity analysis of receiver DSP. BER as a function of the transmission distance for receiver DSP without any equalizer (black square), a T-spaced FFE with 5 taps (red circle), 7 taps (green triangle), 51 taps (dark blue triangle), and full DSP (light blue diamond).

in a BER of $\sim 9.5 \times 10^{-8}$. It can be observed that for transmission of more than 1 km a complex receiver DSP is required. This is because of the power fading caused by chromatic dispersion with direct detection which leads to frequency notches in the broad frequency band of a 100 GBd NRZ signal.

In the next step, we tested the POH MZM with a 112 Gbit/s PAM-4 signal. The BER performance as a function of the received optical power for different transmission distances from BTB to 4 km is depicted in Fig. 5(a). We demonstrate data transmission over 4 km of SMF with a BER below the KP4-FEC limit. The receiver DSP comprises as equalizer algorithms a T/2-spaced FFE with 51 taps, a LUT-MAP with 5 taps, and T-spaced FFE with 101 taps. Fig. 5(b) shows the BER performance as function of transmission distance for different receiver DSP complexities. For data transmission of up to 2 km, no receiver equalizer is required to achieve a BER below the HD-FEC limit. To stay below the KP4-FEC limit the receiver DSP requires a 5 taps T-spaced FFE for 1 km, a 7 taps T-spaced FFE for 2 km, and a 51 taps FFE for 3 km data transmission. To achieve data transmission over 4 km the full receiver DSP is needed. Up to 2 km the increasing transmission distance has almost no influence on

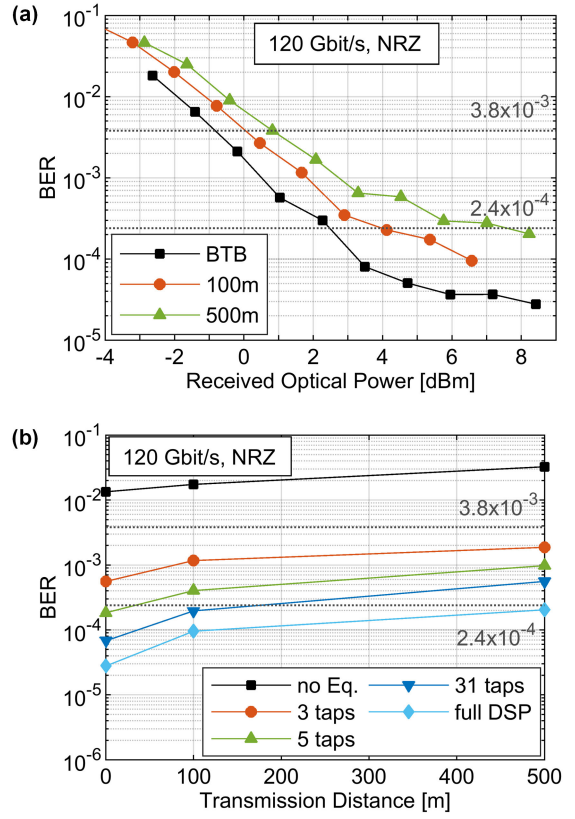


Fig. 6. Experimental results of 120 Gbit/s NRZ OOK signals. As reference the FEC limits at 3.8×10^{-3} and 2.4×10^{-4} (grey dashed) are shown. (a) BER as a function of the received optical power for back-to-back (BTB) (black square), 100 m (red circle), and 500 m (green triangle) transmission. (b) Complexity analysis of receiver DSP. BER as a function of the transmission distance for receiver DSP without any equalizer (black square), a T-spaced FFE with 3 taps (red circle), 5 taps (green triangle), 31 taps (dark blue triangle), and full DSP (light blue diamond).

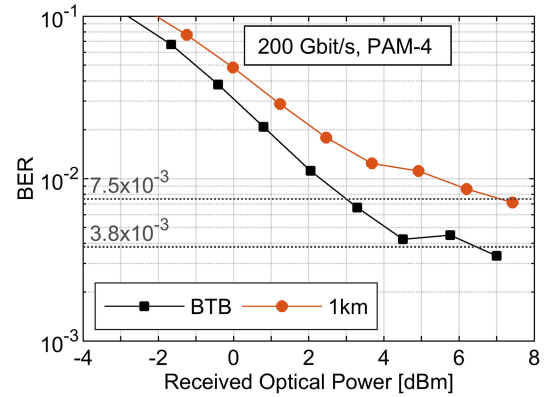


Fig. 7. Experimental results of 200 Gbit/s PAM-4 signals. BER as a function of the received optical power for back-to-back (BTB) (black square) and 1 km (red circle). As reference the FEC thresholds at 7.5×10^{-3} and 3.8×10^{-3} (grey dashed) are shown.

the performance. This is in contrast to 100 Gbit/s NRZ, which suffers already after 1 km from chromatic dispersions induced impairments and is explained by the smaller symbol rate of 56 GBd of the 112 Gbit/s signal.

TABLE I

ANALYSIS OF SIGNAL INTEGRITY FOR DIFFERENT DSP COMPLEXITIES AND DATA RATES OF 100 GBIT/S, 112 GBIT/S, 120 GBIT/S, AND 200 GBIT/S FOR BACK-TO-BACK AS WELL AS TRANSMISSION. THE TRANSMISSION DISTANCE IS INDICATED INSIDE THE EYE DIAGRAMS

	Full DSP		5 taps T-spaced FFE		Without equalization	
	Back-to-back	Transmission	Back-to-back	Transmission	Back-to-back	Transmission
100 Gbit/s NRZ	BER: no errors SNR: 15.21 dB	BER: 8.5×10^{-4} SNR: 10.47 dB	BER: 1.2×10^{-6} SNR: 13.52 dB	BER: 1.9×10^{-5} SNR: 12.33 dB	BER: 5.1×10^{-5} SNR: 11.07 dB	BER: 7.5×10^{-4} SNR: 9.43 dB
112 Gbit/s PAM-4	BER: 2.6×10^{-6} SNR: 20.52 dB	BER: 1.6×10^{-4} SNR: 18.47 dB	BER: 1.7×10^{-4} SNR: 18.03 dB	BER: 8.4×10^{-4} SNR: 16.19 dB	BER: 2.2×10^{-3} SNR: 15.75 dB	BER: 3.7×10^{-3} SNR: 14.84 dB
120 Gbit/s NRZ	BER: 2.9×10^{-5} SNR: 13.08 dB	BER: 1.8×10^{-4} SNR: 11.87 dB	BER: 2.0×10^{-4} SNR: 11.25 dB	BER: 8.8×10^{-4} SNR: 10.09 dB		
200 Gbit/s PAM-4	BER: 3.3×10^{-3} SNR: 15.93 dB	BER: 7.1×10^{-3} SNR: 14.84 dB	BER: 2.0×10^{-2} SNR: 12.66 dB	BER: 4.1×10^{-2} SNR: 11.03 dB		

Transmitter: Intensity modulation
Optical Wavelength: $\sim 1540\text{nm}$
Fiber: SMF-28e+
Receiver: Direct detection
Full DSP: T/2-spaced FFE, LUT-MAP, T-spaced FFE
FFE: Feed-forward equalizer
LUT-MAP: look-up table (LUT) based maximum a posterior (MAP) equalizer

We further increased the symbol rate to 120 GBd with help of an electronic multiplexer. This allows data transmission of a 120 Gbit/s NRZ OOK signal. Fig. 6(a) shows the results as BER performance versus received optical power for different transmission distances. We demonstrate 120 Gbit/s NRZ OOK data transmission over 500 m with a BER below the KP4-FEC limit. The transmission length is significantly reduced, since the symbol rate has a quadratic effect on the strength of the chromatic dispersion. The receiver DSP includes as equalizer algorithms a T/2-spaced FFE with 51 taps, a LUT-MAP with 7 taps, and T-spaced FFE with 101 taps. We also evaluated the receiver DSP complexity requirement for 120 Gbit/s data modulation. Fig. 6(b) shows the results of the complexity analysis as BER performance versus transmission distance for different receiver DSP complexities. It can be seen that a 3 taps T-spaced FFE is sufficient to achieve a BER performance below the HD-FEC limit with a transmission distance of at least up to 500 m.

To achieve a BER performance below the KP4-FEC limit, a T-spaced FFE with 31 taps for 100 m transmission and the full DSP for 500 m transmission were required. For 120 Gbit/s signals, in all cases at least a simple equalizer was required because of the limiting electronic bandwidth, especially of the real-time oscilloscope of about 63 GHz. Besides, we didn't apply any pre-distortion to compensate any bandwidth limitations from the electronics in the case of Tx-B.

Finally, we increased the data rate to 200 Gbit/s with the transmitter scenario Tx-A. The signal has a symbol rate of 100 GBd and uses PAM-4 as modulation format. Fig. 7 shows the results of the BER as function of the received optical power for the BTB scenario and transmission over 1 km SMF. It can be seen that in the BTB scenario a BER below the HD-FEC can be achieved. After 1 km transmission the BER stays below a 10% overhead HD staircase FEC [43] limit of 7.5×10^{-3} . The receiver DSP includes a T/2-spaced FFE with 101 taps, a LUT-MAP with 7 taps, and T-spaced FFE with 101 taps. In case of the 200 Gbit/s signal we did not analyze the DSP complexity since only DSP with high complexity was sufficient to achieve BERs below the HD-FEC limit.

C. Eye Diagrams

Table I highlights the eye diagrams captured at the receiver which are a qualitative way to evaluate the signal integrity. The eye diagrams are obtained after the receiver DSP and are digitally interpolated with 10^6 symbols and a raised cosine pulse shape with a roll-off factor of one. The given BER is calculated for $\sim 1.5 \times 10^7$ bits. Additionally, we display the signal-to-noise ratio (SNR) which is digitally estimated on the symbol level. The eye diagrams are given for the four different line rates 100 Gbit/s NRZ, 112 Gbit/s PAM-4, 120 Gbit/s NRZ, and 200 Gbit/s

PAM-4 which are separated by rows. The three different main columns represent the different cases of DSP complexity that are full DSP, single 5 taps T-space FFE, and without any equalization. Besides, the columns distinguish between BTB and transmission.

In the case of the DSP complexity without any equalization at the receiver the DSP applies only timing recovery and normalization onto the digitized waveform. It can be observed that data transmission of up to 1 km and 2 km can be achieved for 100 Gbit/s and 112 Gbit/s with a BER below the HD-FEC threshold. It confirms that the plasmonic modulator does not introduce any bandwidth limitations.

V. CONCLUSION AND OUTLOOK

We have demonstrated 200 Gbit/s PAM-4 data transmission with a plasmonic modulator in an intensity modulation direct detection optical interconnect with 1 km single mode fiber at a wavelength of 1540 nm and with high DSP complexity. Besides, we demonstrated 100 Gbit/s NRZ, 112 Gbit/s PAM-4, and 120 Gbit/s NRZ data transmission over 2 km, 4 km, and 500 m of single mode fiber with a BER performance below the KP4 threshold of $2.4 - 10^{-4}$. The required complexity of the receiver DSP has been investigated. We have shown that data transmission of 100 Gbit/s and 112 Gbit/s over 1 km and 2 km of single mode fiber without equalization at the receiver and a BER below the HD-FEC threshold of 3.8×10^{-3} can be achieved. Furthermore, we measured the electro-optic frequency response of the plasmonic modulator and did not observe any indication of a magnitude roll-off for frequencies up to 108 GHz.

The receiver DSP complexity studies and the frequency response measurement show that the plasmonic modulator does not introduce any additional low-pass characteristic in the IM-DD transceiver system. This underlines the large frequency response of at least 170 GHz from previous measurements [20].

To achieve more robustness towards chromatic dispersion even with large symbol rates, the IM-DD system with the POH can also be shifted towards the O-band with a wavelength of 1310 nm [7]. This results in an additional advantage of increased nonlinearities and thus an increased modulation efficiency [44]. Shifting the operation wavelength to 1310 nm reduces the voltage-length product and thus, when keeping the V_π , constant, the length of the active region that consequently lowers the insertion losses.

ACKNOWLEDGMENT

This paper was partly carried out at the BRNC and FIRST of ETH Zurich. The authors would like to thank Aldo Rossi for technical support.

REFERENCES

- [1] P. J. Winzer and D. T. Neilson, "From scaling disparities to integrated parallelism: A decathlon for a decade," *J. Lightw. Technol.*, vol. 35, no. 5, pp. 1099–1115, Mar. 2017.
- [2] J. M. Estaran *et al.*, "140/180/204-Gbaud OOK transceiver for inter- and intra-data center connectivity," *J. Lightw. Technol.*, vol. 37, no. 1, pp. 178–187, Jan. 2019.
- [3] C. Minkenberg *et al.*, "Reimagining datacenter topologies with integrated silicon photonics," *J. Opt. Commun. Netw.*, vol. 10, pp. B126–B139, Jul. 2018.
- [4] A. V. Krishnamoorthy *et al.*, "Computer systems based on silicon photonic interconnects," *Proc. IEEE*, vol. 97, no. 7, pp. 1337–1361, Jul. 2009.
- [5] O. Ozolins *et al.*, "100 GHz externally modulated laser for optical interconnects," *J. Lightw. Technol.*, vol. 35, no. 6, pp. 1174–1179, Mar. 2017.
- [6] J. Verbist *et al.*, "Real-time 100 Gb/s NRZ and EDB transmission with a GeSi electro-absorption modulator for short-reach optical interconnects EAM," *J. Lightw. Technol.*, vol. 36, no. 1, pp. 90–96, Jan. 2018.
- [7] S. Kanazawa *et al.*, "214-Gb/s 4-PAM operation of flip-chip interconnection EADFB laser module," *J. Lightw. Technol.*, vol. 35, no. 3, pp. 418–422, Feb. 2017.
- [8] S. Lange *et al.*, "100 GBd intensity modulation and direct detection with an InP-based monolithic DFB laser Mach-Zehnder modulator," *J. Lightw. Technol.*, vol. 36, no. 1, pp. 97–102, Jan. 2018.
- [9] X. Chen *et al.*, "All-electronic 100-GHz bandwidth digital-to-analog converter generating PAM signals up to 190 GBaud," *J. Lightw. Technol.*, vol. 35, no. 3, pp. 411–417, Feb. 2017.
- [10] C. Wang *et al.*, "Integrated lithium niobate electro-optic modulators operating at CMOS-compatible voltages," *Nature*, vol. 562, pp. 101–104, Sep. 2018.
- [11] K. Schuh, E. Lach, and B. Junginger, "100 Gbit/s ETDM transmission system based on electronic multiplexing transmitter and demultiplexing receiver," in *Proc. Eur. Conf. Opt. Commun.*, Cannes, France, Sep. 2006, pp. 1–2.
- [12] E. Lach and K. Schuh, "Recent advances in ultrahigh bit rate ETDM transmission systems," *J. Lightw. Technol.*, vol. 24, no. 12, pp. 4455–4467, Dec. 2006.
- [13] Y. Ogiso *et al.*, "100 Gb/s and 2 V V_π InP Mach-Zehnder modulator with an n-i-p-n heterostructure," *Electron. Lett.*, vol. 52, pp. 1866–1867, Oct. 2016.
- [14] S. Wolf *et al.*, "Silicon-Organic Hybrid (SOH) Mach-Zehnder modulators for 100 Gbit/s on-off keying," *Sci. Rep.*, vol. 8, Apr. 2018, Art. no. 2598.
- [15] V. Katopodis *et al.*, "Serial 100 Gb/s connectivity based on polymer photonics and InP-DHBT electronics," *Opt. Express*, vol. 20, pp. 28538–28543, Dec. 2012.
- [16] C. Haffner *et al.*, "Plasmonic organic hybrid modulators—Scaling highest speed photonics to the microscale," *Proc. IEEE*, vol. 104, no. 12, pp. 2362–2379, Dec. 2016.
- [17] C. Haffner *et al.*, "All-plasmonic Mach-Zehnder modulator enabling optical high-speed communication at the microscale," *Nature Photon.*, vol. 9, pp. 525–528, Jul. 2015.
- [18] M. Ayata *et al.*, "High-speed plasmonic modulator in a single metal layer," *Science*, vol. 358, pp. 630–632, Nov. 2017.
- [19] W. Heni *et al.*, "108 Gbit/s Plasmonic Mach-Zehnder Modulator with >70-GHz electrical bandwidth," *J. Lightw. Technol.*, vol. 34, no. 2, pp. 393–400, Jan. 2016.
- [20] C. Hoessbacher *et al.*, "Plasmonic modulator with >170 GHz bandwidth demonstrated at 100 GBd NRZ," *Opt. Express*, vol. 25, pp. 1762–1768, Jun. 2017.
- [21] B. Baeuerle *et al.*, "Driver-less sub 1 V pp operation of a plasmonic-organic hybrid modulator at 100 GBd NRZ," in *Proc. Opt. Fiber Commun. Conf. Expo.*, San Diego, CA, USA, Mar. 2018, Paper M2I.1.
- [22] W. Heni *et al.*, "High speed plasmonic modulator array enabling dense optical interconnect solutions," *Opt. Express*, vol. 23, pp. 29746–29757, Nov. 2015.
- [23] C. Hoessbacher *et al.*, "Optical interconnect solution with plasmonic modulator and Ge photodetector array," *IEEE Photon. Technol. Lett.*, vol. 29, no. 21, pp. 1760–1763, Nov. 2017.
- [24] U. Koch *et al.*, "Ultra-compact terabit plasmonic modulator array," *J. Lightw. Technol.*, to be published.
- [25] S. Bhoja, V. Parthasarathy, and Z. Wang, "FEC codes for 400 Gbps 802.3bs 400 GbE Task Force, Plenary Meeting Material, Macau, 2014. [Online]. Available: http://www.ieee802.org/3/bs/public/14_11/parthasarathy_3bs_01a_1114.pdf
- [26] B. Baeuerle *et al.*, "Plasmonic-organic hybrid modulators for optical interconnects beyond 100G/ λ ," in *Proc. Conf. Lasers Electro-Optics*, San Jose, CA, USA, May 2018, pp. 1–2.
- [27] W. Heni *et al.*, "Silicon-organic and plasmonic-organic hybrid photonics," *ACS Photon.*, vol. 4, pp. 1576–1590, Jul. 2017.
- [28] T. Watanabe, M. Ayata, U. Koch, Y. Fedoryshyn, and J. Leuthold, "Perpendicular grating coupler based on a blazed antiback-reflection structure," *J. Lightw. Technol.*, vol. 35, no. 21, pp. 4663–4669, Nov. 2017.

- [29] A. Melikyan *et al.*, "High-speed plasmonic phase modulators," *Nature Photon.*, vol. 8, pp. 229–233, Feb. 2014.
- [30] D. L. Elder *et al.*, "Effect of rigid bridge-protection units, quadrupolar interactions, and blending in organic electro-optic chromophores," *Chem. Mater.*, vol. 29, pp. 6457–6471, Aug. 2017.
- [31] S. Ummethala *et al.*, "Terahertz-to-optical conversion using a plasmonic modulator," in *Proc. Conf. Lasers Electro-Optics*, San Jose, CA, USA, 2018, pp. 1–2.
- [32] C. Kieninger *et al.*, "Ultra-high electro-optic activity demonstrated in a silicon-organic hybrid modulator," *Optica*, vol. 5, pp. 739–748, Jun. 2018.
- [33] B. H. Robinson *et al.*, "Optimization of plasmonic-organic hybrid electro-optics," *J. Lightw. Technol.*, vol. 36, no. 21, pp. 5036–5047, Nov. 2018.
- [34] C. Kieninger *et al.*, "Demonstration of long-term thermally stable silicon-organic hybrid modulators at 85 °C," *Opt. Express*, vol. 26, pp. 27955–27964, 2018.
- [35] K. Schuh *et al.*, "100 GSa/s BiCMOS DAC supporting 400 Gb/s dual channel transmission," in *Proc. 42nd Eur. Conf. Opt. Commun.*, 2016, pp. 1–3.
- [36] S. Randel *et al.*, "All-electronic flexibly programmable 864-Gb/s single-carrier PDM-64-QAM," in *Proc. Conf. Opt. Fiber Commun.*, Mar. 2014, pp. 1–3.
- [37] C. Uhl, H. Hettrich, and M. Möller, "Design considerations for a 100 Gbit/s SiGe-BiCMOS power multiplexer with 2 Vpp differential voltage swing," *IEEE J. Solid-State Circuits*, vol. 53, no. 9, pp. 2479–2487, Sep. 2018.
- [38] Y. Cai *et al.*, "Experimental demonstration of coherent MAP detection for nonlinearity mitigation in long-haul transmissions," in *Proc. Conf. Opt. Fiber Commun.*, San Diego, CA, USA, Mar. 2010, pp. 1–3.
- [39] A. Rezania and J. C. Cartledge, "Transmission performance of 448 Gb/s single-carrier and 1.2 Tb/s three-carrier superchannel using dual-polarization 16-QAM with fixed LUT based MAP detection," *J. Lightw. Technol.*, vol. 33, no. 23, pp. 4738–4745, Dec. 2015.
- [40] H. Mardoyan *et al.*, "84-, 100-, and 107-GBd PAM-4 intensity-modulation direct-detection transceiver for datacenter interconnects," *J. Lightw. Technol.*, vol. 35, no. 6, pp. 1253–1259, Mar. 2017.
- [41] ITU-T *Recommendation G.975.1*, International Telecommunications Union, Geneva, Switzerland, 2004.
- [42] J. Cho, C. Xie, and P. J. Winzer, "Analysis of soft-decision FEC on non-AWGN channels," *Opt. Express*, vol. 20, pp. 7915–7928, 2012.
- [43] L. M. Zhang and F. R. Kschischang, "Staircase codes with 6% to 33% overhead," *J. Lightw. Technol.*, vol. 32, no. 10, pp. 1999–2002, May 2014.
- [44] C. Haffner *et al.*, "Harnessing nonlinearities near material absorption resonances for reducing losses in plasmonic modulators," *Opt. Mater. Express*, vol. 7, pp. 2168–2181, Jul. 2017.

Authors' biographies not available at the time of publication.